Electronic Supplementary Material (ESI) for Journal of Materials Chemistry C.
This journal is © The Royal Society of Chemistry 2021

Novel 12,12-Dimethyl-7,12-dihydrobenzo[*a*]acridine as a Deep-Blue Emitting Chromophore for OLEDs with Narrow-Band Emission and Suppressed Efficiency Roll-Off

Xu Qiu,[2,3‡] Lei Xu,[2‡] Shian Ying,[4] Xiyun Ye,[2] Pei Xu,[2] Bohan Wang,[2] Dehua Hu, [1,2*] Dongge Ma,[2*] Yuguang Ma[2*]

1. School of Chemical Engineering and Light Industry, Guangdong University of Technology, Guangzhou 510006, China. E-mail: msdhhu@scut.edu.cn;

2. Institute of Polymer Optoelectronic Materials and Devices, State Key Laboratory of Luminescent Materials and Devices, South China University of Technology, Guangzhou 510640, China.

E-mail: msdgma@scut.edu.cn; ygma@scut.edu.cn

3. College of Materials Science and Engineering, Shandong University of Science and Technology, Qingdao 266590, China.

4. School of Polymer Science and Engineering, Qingdao University of Science and Technology, Qingdao, 266042, China.

Contents

SI-1. General information

Measurements

^{1}H and ^{13}C NMR spectra were recorded on a Bruker AC500 (500 MHz) spectrometer at 298 K by utilizing $CDCl_3$ as the solvent and tetramethylsilane (TMS) as the internal standard. Mass spectral data were obtained using a Finnigan 4021C gas chromatography (GC)-mass spectrometry (MS) instrument. Elemental analysis was performed on a PerkinElmer 2400. UV-vis absorption spectra were recorded on a Hitachi U-4100 spectrophotometer. Fluorescence measurements were carried out with a Hitachi F-4600 spectrophotometer. The quantum efficiencies of solutions and solid films were carried out with FLS980 Spectrometer with a calibrated integrating sphere. Thermal gravimetric analysis (TGA) was undertaken on a PerkinElmer thermal analysis system at a heating rate of 10 ^{o}C min^{-1} and a nitrogen flow rate of 40 mL min^{-1}. Differential scanning calorimetry (DSC) was performed on a NETZSCH (DSC-204) unit at a heating rate of 10 ^{o}C min^{-1} under nitrogen. Cyclic voltammetry (CV) was performed using a BAS 100W (Bioanalytical Systems), using a glass carbon disk (diameter = 3 mm) as the working electrode, a platinum wire with a porous ceramic wick as the auxiliary electrode, and Ag/Ag^{+} as the reference electrode standardized by the redox couple ferrocenium/ferrocene. Anhydrous *N,N*-dimethylformamide (DMF) and dichloromethane (CH_2Cl_2) containing 0.1 M tetrakis(n-butyl)-ammonium hexafluorophosphate (NBu_4PF_6) as the supporting electrolyte were used as solvents under a nitrogen atmosphere. All solutions were purged with a nitrogen stream for 10 min before measurements. The procedure was performed at room temperature, and a

nitrogen atmosphere was maintained over the solution during measurements. A scan rate of 50 mV s^{-1} was applied.

Theoretical calculation

Density functional theory (DFT) calculations were performed using Gaussian 09-B01 program Package. The geometry at ground state of the molecule in the gas phase was optimized under the framework of DFT at B3LYP/6-31G (d, p) level and the single point properties at ground state such as molecule orbits were calculated at the level of M06-2X/def2-TZVP. On the basis of the optimized configuration of the ground state (S_0), the high excitation energy levels of singlet and triplet states were evaluated using TD-M062X/6-31+G (d, p). In order to gain further insight into the character of excited states, natural transition orbitals (NTOs) were evaluated for first five singlet and triplet states. The NTOs were generated using the Multiwfn program from the density matrices of TDDFT calculations. The SOCs between different S_m and T_n states were calculated with the PySOC program using the linear-response (LR) methods based on the excited-state wave functions obtained from TDDFT calculations above.

Device fabrication

Indium−tin oxide (ITO) coated glass with a sheet resistance of 15–20 Ω cm^{-2} was used as the substrate. Before device fabrication, the ITO glass substrates were cleaned with acetone, detergent, deionized water, and isopropanol, dried in an oven at 120 ^{o}C, and treated with UV-zone for 20 min. After that, the samples were transferred into a deposition system. The devices were fabricated by the multiple source organic molecular beam deposition method in a vacuum at a pressure of 4×10^{-6} mbar.

Evaporation rates of 0.4 Å s^{-1} for the organic materials and 1–4 Å s^{-1} for the metal electrodes were applied. The thickness of each deposition layer was monitored using a quartz crystal thickness/ratio monitor (STM-100/MF, Sycon). The EL spectra were measured using a PR650 fluorescence spectrophotometer. The current density–voltage–luminance (*J–V–L*) characteristics were performed simultaneously by using a computer-controlled source meter (Keithley 2400) equipped with a light intensity meter LS-110. The EQEs were calculated from the luminance, current density and EL spectrum, assuming a Lambertian distribution. All the results of devices were measured in the forward-viewing direction without any out-coupling enhancement techniques.

SI-2. Synthesis

All reagents and solvents (including super-dry solvents) used for the synthesis and characterization were purchased from Aldrich Chemical Co., or Energy Chemical Co., China and used without further purification. Toluene was distilled over metallic sodium and before use.

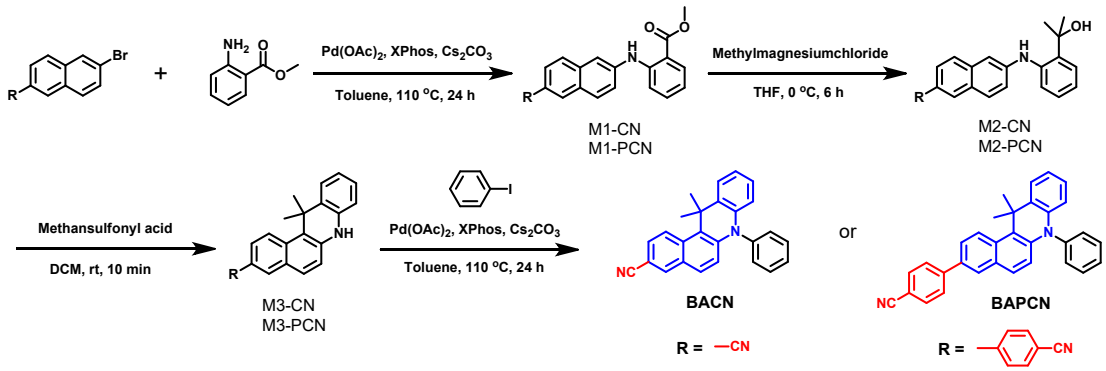

Scheme S1. Synthesis route of BACN and BAPCN.

Methyl 2-((6-cyanonaphthalen-2-yl)amino)benzoate (M1-CN)

Commercially available 6-bromo-2-naphthonitrile (5.00 g, 21.54 mmol), methyl 2-

aminobenzoate (3.58 g, 23.70 mmol), $Pd(OAc)_2$ (0.24 g, 1.08 mmol), XPhos (1.03 g, 2.15 mmol) and $CsCO_3$ (10.50 g, 32.32 mmol) were dissolved in dry toluene (100 mL), and then the resulted mixture was stirred at a temperature of 110 ^oC for 24 hours. After cooling down room temperature, the reaction was quenched using water, and then an extraction process was performed thereon three times using ethyl acetate. A separated organic layer was dried using anhydrous magnesium sulfate and concentrated under reduced pressure. The given residue was purified through silica gel column chromatography using dichloromethane/petroleum ether (1/2) as eluent to give the product as a pale yellow solid product (6.50 g, 89%). ^1H NMR (500 MHz, $CDCl_3$) δ 9.81 (s, 1H), 8.13 (s, 1H), 8.03 (dd, J = 8.0, 1.6 Hz, 1H), 7.83 (d, J = 8.9 Hz, 1H), 7.74 (d, J = 8.6 Hz, 1H), 7.66 (d, J = 2.1 Hz, 1H), 7.58 – 7.51 (m, 2H), 7.50 – 7.40 (m, 2H), 6.90 (m, 1H), 3.93 (s, 3H). MS (APCI): m/z: 302.2 $[M + 1]^+$.

6-((2-(2-hydroxypropan-2-yl)phenyl)amino)-2-naphthonitrile (M2-CN)

The M1-CN (4.00 g, 13.25 mmol) was diluted in 100 mL of dry tetrahydrofuran, and then at a temperature of 0 ^oC, 13.2 mL (39.74 mmol) of methylmagnesiumchloride (3 mol L^{-1}) was slowly added dropwise for over 20 min to the solution. After 6 hours of stirring, the reaction was quenched using ammonium chloride, and then an extraction process was performed three times using ethyl acetate. A separated organic layer was dried using anhydrous magnesium sulfate and concentrated under reduced pressure. The given residue was purified through silica gel column chromatography using petroleum ether/ethyl acetate (3/1) as eluent to give the product as a faint yellow solid product (3.24 g, 81%). ^1H NMR (500 MHz, $CDCl_3$) δ 8.05 (s, 1H), 7.73 (d, J = 8.9 Hz,

1H), 7.61 (d, J = 8.6 Hz, 1H), 7.54 (dd, J = 8.0, 1.2 Hz, 1H), 7.46 (dd, J = 8.5, 1.6 Hz, 1H), 7.38 (d, J = 2.2 Hz, 1H), 7.36 (dd, J = 3.7, 1.8 Hz, 1H), 7.30 (dt, J = 8.8, 1.9 Hz, 2H), 7.01 (td, J = 7.7, 1.2 Hz, 1H), 4.08 (s, 1H), 3.48 (s, 1H), 1.69 (s, 6H). MS (APCI): m/z: 302.1 $[M + 1]^+$.

12,12-dimethyl-7,12-dihydrobenzo[a]acridine-3-carbonitrile (M3-CN)

The M2-CN (3.00 g, 9.93 mmol) was diluted in 100 mL of dichloromethane, and the 0.64 mL of methansulfonyl acid was slowly added dropwise in the solution. 10 minutes after the addition, the reaction was quenched using triethylamine. The solution was concentrated under reduced pressure. The given residue was purified through silica gel column chromatography using petroleum ether/dichloromethane (2/3) as eluent to give the product as a faint yellow solid product (2.20 g, 78%). ^{1}H NMR (500 MHz, $CDCl_3$) δ 8.40 (s, 1H), 8.00 (s, 1H), 7.52 (dd, J = 24.4, 8.4 Hz, 2H), 7.39 (s, 1H), 7.21 – 6.11 (m, 4H), 4.03 (s, 1H)2.13 (s, 6H). MS (APCI): m/z: 284.3 $[M + 1]^+$.

12,12-dimethyl-7-phenyl-7,12-dihydrobenzo[a]acridine-3-carbonitrile (BACN)

The M3-CN (1.50 g, 5.28 mmol), iodobenzene (1.29 g, 6.34 mmol), $Pd(OAc)_2$ (0.06 g, 0.26 mmol), XPhos (0.25 g, 0.53 mmol) and $CsCO_3$ (2.57 g, 7.92 mmol) was dissolved in 80 mL dry toluene, and then the resulted mixture was stirred at a temperature of 110 ^oC for 24 hours. After cooling down room temperature, the reaction was quenched using water, and then an extraction process was performed thereon three times using dichloromethane. A separated organic layer was dried using anhydrous magnesium sulfate and concentrated under reduced pressure. The given residue was purified through silica gel column chromatography using dichloromethane/petroleum ether

(2/3) as eluent to give the product as a pale yellow solid product (1.59 g, 84%). ^{1}H NMR (500 MHz, $CDCl_3$) δ 8.51 (d, J = 9.3 Hz, 1H), 7.97 (d, J = 1.9 Hz, 1H), 7.71 – 7.61 (m, 2H), 7.58 – 7.48 (m, 2H), 7.46 (dd, J = 7.7, 1.7 Hz, 1H), 7.37 (d, J = 9.1 Hz, 1H), 7.30 (dt, J = 8.4, 1.8 Hz, 2H), 6.98 – 6.86 (m, 2H), 6.55 (d, J = 9.2 Hz, 1H), 6.06 (dd, J = 8.1, 1.4 Hz, 1H), 2.27 (s, 6H). ^{13}C NMR (125 MHz, $CDCl_3$) δ 141.31, 140.06, 137.63, 135.27, 134.04, 133.06, 131.38, 131.12, 129.28, 128.66, 128.64, 128.04, 126.98, 126.45, 125.90, 121.54, 120.27, 119.66, 118.65, 114.46, 104.75, 36.49, 34.32. MS (APCI): m/z: 360.4 $[M + 1]^+$. Anal. calcd for C26H20N2: C, 86.64; H, 5.59; N, 7.77. Found: C, 86.67; H, 5.60; N, 7.73.

methyl 2-((6-(4-cyanophenyl)naphthalen-2-yl)amino)benzoate (M1-PCN)

4-(6-bromonaphthalen-2-yl)benzonitrile (2.50 g, 8.12 mmol), methyl 2-aminobenzoate (1.47 g, 9.74 mmol), $Pd(OAc)_2$ (0.09 g, 0.41 mmol), XPhos (0.39 g, 0.81 mmol) and $CsCO_3$ (3.96 g, 12.18 mmol) were dissolved in dry toluene (50 mL), and then the resulted mixture was stirred at a temperature of 110 ^{o}C for 24 hours. After cooling down room temperature, the reaction was quenched using water, and then an extraction process was performed thereon three times using ethyl acetate. A separated organic layer was dried using anhydrous magnesium sulfate and concentrated under reduced pressure. The given residue was purified through silica gel column chromatography using dichloromethane/petroleum ether (3/2) as eluent to give the product as a pale yellow solid product (2.67 g, 87%). ^{1}H NMR (500 MHz, $CDCl_3$) δ 9.73 (s, 1H), 8.05 – 7.98 (m, 2H), 7.86 (d, J = 8.7 Hz, 1H), 7.84 – 7.77 (m, 3H), 7.77 – 7.72 (m, 2H), 7.67 (dd, J = 8.5, 2.0 Hz, 2H), 7.44 (td, J = 9.1, 8.6, 1.7 Hz, 2H), 7.38 (ddd, J = 8.5, 7.0, 1.7

Hz, 1H), 6.82 (ddd, J = 8.2, 7.0, 1.2 Hz, 1H), 3.93 (s, 3H). MS (APCI): m/z: 378.3 [M + 1]$^{+}$.

4-(6-((2-(2-hydroxypropan-2-yl)phenyl)amino)naphthalen-2-yl)benzonitrile (M2-PCN)

The M1-PCN (2.00 g, 5.29 mmol) was diluted in 60 mL of dry tetrahydrofuran, and then at a temperature of 0 ^{o}C, 5.29 mL (15.87 mmol) of methylmagnesiumchloride (3 mol L^{-1}) was slowly added dropwise for over 20 min to the solution. After 6 hours of stirring, the reaction was quenched using ammonium chloride, and then an extraction process was performed three times using ethyl acetate. A separated organic layer was dried using anhydrous magnesium sulfate and concentrated under reduced pressure. The given residue was purified through silica gel column chromatography using dichloromethane/petroleum ether (4/1) as eluent to give the product as a faint yellow solid product (1.58 g, 79%). ^{1}H NMR (500 MHz, $CDCl_3$) δ 7.94 (d, J = 1.9 Hz, 1H), 7.86 – 7.76 (m, 4H), 7.76 – 7.68 (m, 3H), 7.67 – 7.59 (m, 1H), 7.53 (dd, J = 8.1, 1.3 Hz, 1H), 7.45 (d, J = 2.2 Hz, 1H), 7.36 – 7.27 (m, 2H), 6.97 (td, J = 7.6, 1.3 Hz, 1H), 4.02 (s, 1H), 3.47 (s, 1H), 1.71 (s, 6H). MS (APCI): m/z: 378.2 [M + 1]$^{+}$.

4-(12,12-dimethyl-7,12-dihydrobenzo[a]acridin-3-yl)benzonitrile (M3-PCN)

The M2-PCN (2.00 g, 5.29 mmol) was diluted in 80 mL of dichloromethane, and the 0.34 mL of methansulfonyl acid was slowly added dropwise in the solution. 10 minutes after the addition, the reaction was quenched using triethylamine. The solution was concentrated under reduced pressure. The given residue was purified through silica gel column chromatography using petroleum ether/dichloromethane (1/1) as eluent to give

the product as a faint yellow solid product (1.43 g, 75%). ^{1}H NMR (500 MHz, $CDCl_3$) δ 8.47 (s, 2H), 8.02 – 7.53 (m, 7H), 7.41 (s, 1H), 7.07 (s, 1H), 6.80 (s, 2H), 4.02 (s, 1H), 2.19 (s, 6H). MS (APCI): m/z: 360.4 $[M + 1]^+$.

4-(12,12-dimethyl-7-phenyl-7,12-dihydrobenzo[a]acridin-3-yl)benzonitrile (BAPCN)

The M3-PCN (1.6 g, 4.44 mmol), iodobenzene (1.09 g, 5.33 mmol), $Pd(OAc)_2$ (0.05 g, 0.22 mmol), XPhos (0.21 g, 0.44 mmol) and $CsCO_3$ (2.17 g, 6.67 mmol) was dissolved in 80 mL dry toluene, and then the resulted mixture was stirred at a temperature of 110 ^{o}C for 24 hours. After cooling down room temperature, the reaction was quenched using water, and then an extraction process was performed thereon three times using dichloromethane. A separated organic layer was dried using anhydrous magnesium sulfate and concentrated under reduced pressure. The given residue was purified through silica gel column chromatography using dichloromethane/petroleum ether (1/1) as eluent to give the product as a pale yellow solid product (1.57 g, 81%). ^{1}H NMR (500 MHz, $CDCl_3$) δ 8.58 (d, J = 9.3 Hz, 1H), 7.86 (d, J = 2.2 Hz, 1H), 7.82 – 7.76 (m, 2H), 7.76 – 7.70 (m, 2H), 7.69 – 7.61 (m, 3H), 7.53 (tt, J = 7.1, 1.2 Hz, 1H), 7.50 – 7.45 (m, 1H), 7.43 (d, J = 9.1 Hz, 1H), 7.33 (dt, J = 8.3, 1.7 Hz, 2H), 6.95 – 6.86 (m, 2H), 6.51 (d, J = 9.1 Hz, 1H), 6.11 – 6.04 (m, 1H), 2.32 (s, 6H). ^{13}C NMR (125 MHz, $CDCl_3$) δ 145.14, 141.84, 138.30, 138.11, 133.04, 132.62, 132.14, 132.05, 131.38, 131.24, 130.55, 128.69, 128.38, 128.07, 127.81, 127.28, 127.14, 126.31, 124.04, 120.94, 120.03, 119.12, 118.02, 114.21, 110.34, 36.61, 34.32. MS (APCI): m/z: 436.3 $[M + 1]^+$. Anal. calcd for C32H24N2: C, 88.04; H, 5.54; N, 6.42. Found: C, 88.01; H, 5.58; N, 6.41.

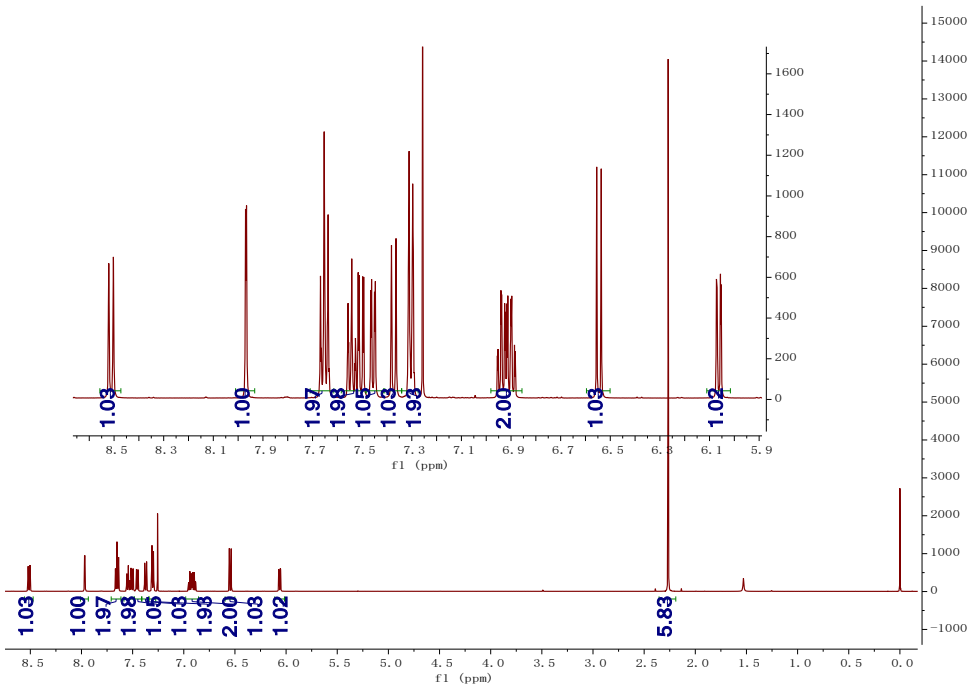

Fig. S1. ^{1}H NMR spectrum of BACN in $CDCl_3$.

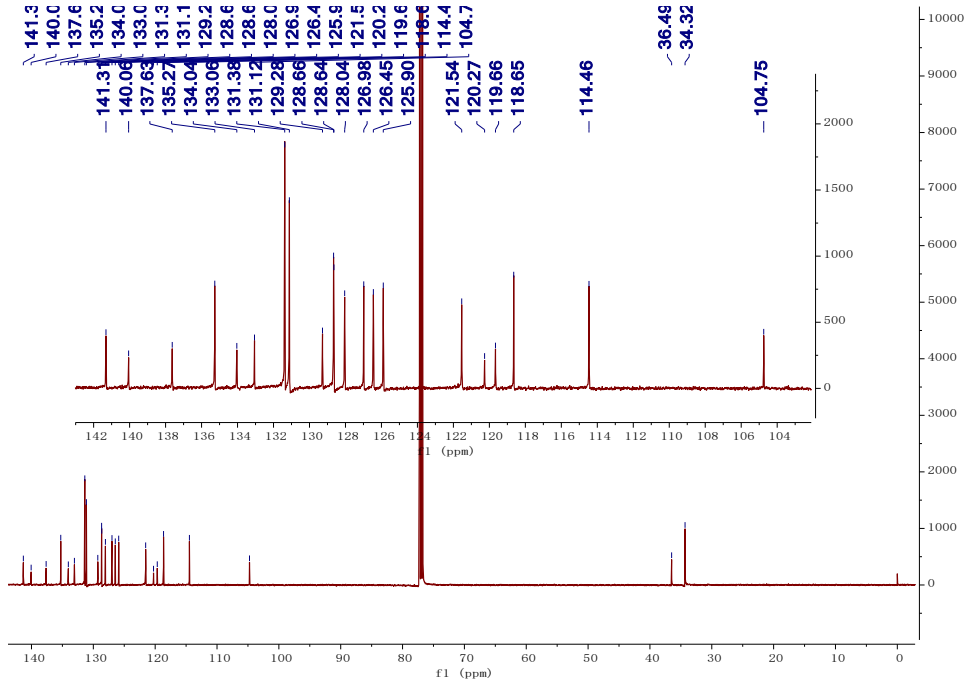

Fig. S2. ^{13}C NMR spectrum of BACN in $CDCl_3$.

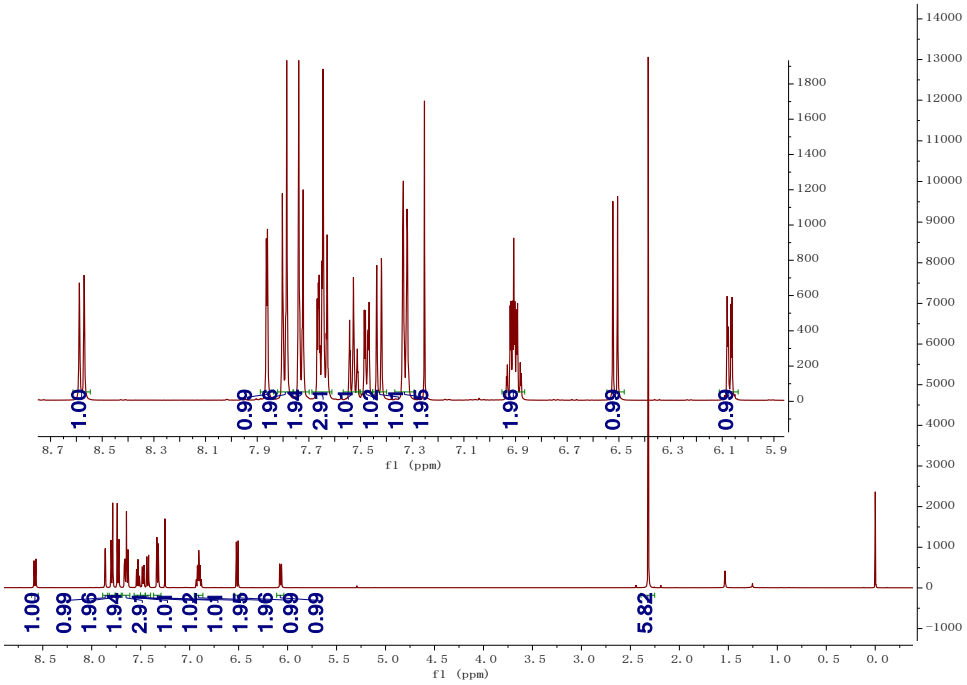

Fig. S3. ^{1}H NMR spectrum of BAPCN in $CDCl_3$.

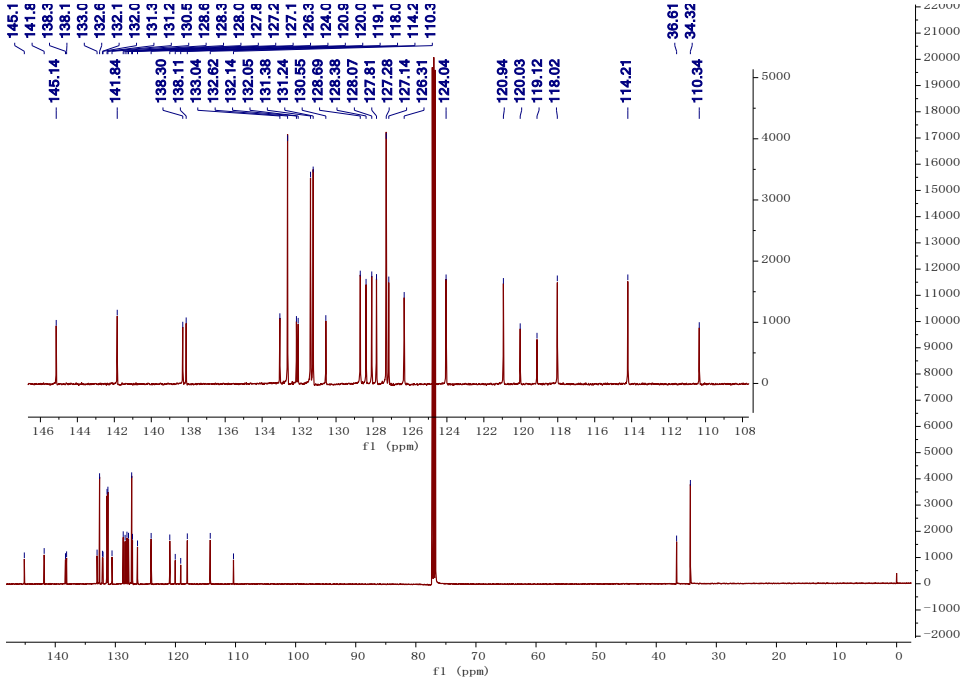

Fig. S4. ^{13}C NMR spectrum of BAPCN in $CDCl_3$.

SI-3. Thermal and electrochemical properties

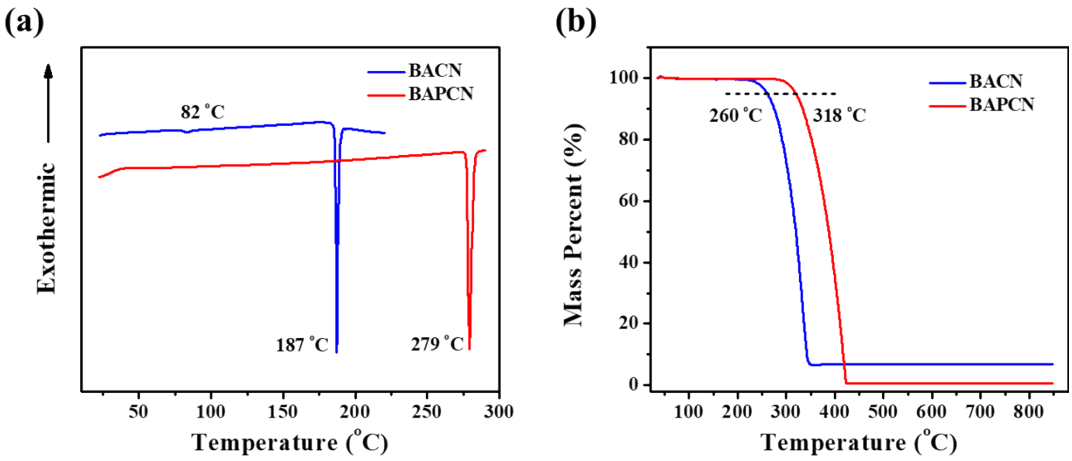

Fig. S5. (a) DSC and (b) TGA curves of BACN and BAPCN.

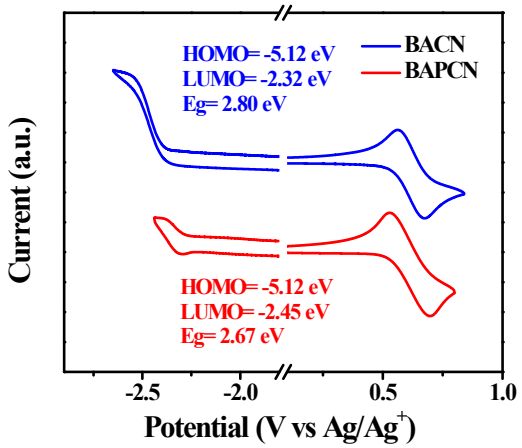

Fig. S6. Cyclic voltammetry curves of BACN and BAPCN.

The electrochemical properties of BACN and BAPCN were obtained from the cyclic voltammetry (CV) measurements. From the onset of the oxidation potential, the highest occupied molecular orbitals (HOMO) energy is estimated to be -5.12 eV for both BACN and BAPCN. Moreover, the lowest unoccupied molecular orbitals (LUMO) energy could be obtained from the onset of reduction potentials. The LUMOs are -2.32 eV and -2.45 eV for BACN and BAPCN, respectively. Therefore, the energy gaps (E_gs) of BACN and BAPCN could be calculated to be 2.80 and 2.67 eV, respectively. The detailed parameters in the Table 1 in main article.

SI-4. Crystal data

Table S1. Crystal data and structural refinement for BACN and BAPCN crystals.

Compound name	BACN	BAPCN
Compound reference	clear light yellow crystal	yellow crystal
Chemical formula	C26 H20 N2	C32 H24 N2
Formula weight	360.44	436.53
Crystal system	Monoclinic	Monoclinic
a/Å	15.8871(4)	33.6072(7)
b/ Å	8.51966(11)	7.93808(16)
c/ Å	16.1057(4)	16.8859(3)
α/°	90	90
β/°	119.369(3)	101.9277(19)
γ/°	90	90
Unit cell volume/ Å3	1899.78(8)	4407.48(15)
Temperature/K	100.1(9)	100.0(6)
Space group	P-2	C-2
Z	4	8
Density (calculated) /g cm^{-3}	1.260	1.316
F(000)	760	1840
Theta range for data collection	3.201 to 67.073 deg.	4.1890 to 73.2830 deg.
Index ranges	-18<=h<=18, -10<=k<=10, -18<=l<=19	-37<=h<=40, -7<=k<=9, -15<=l<=20
Reflections measured	3390	3948
Independent reflections	3024	3550
Rint	0.0289	0.0199
Absorption correction	multi-scan	multi-scan
Refinement method	none	none
Data / restraints / parameters	3390 / 0 / 255	3948 / 0 / 309
Goodness-of-fit on F^2	1.045	1.039
Final R_1 values ($I > 2\sigma(I)$)	0.0341	0.0338
Final $wR(F^2)$ values ($I > 2\sigma(I)$)	0.0909	0.0914
Final R_1values (all data)	0.0380	0.0375
Final $wR(F^2)$ values (all data)	0.0939	0.0940
CCDC number	2042850	2042752

SI-5. Theoretical calculations

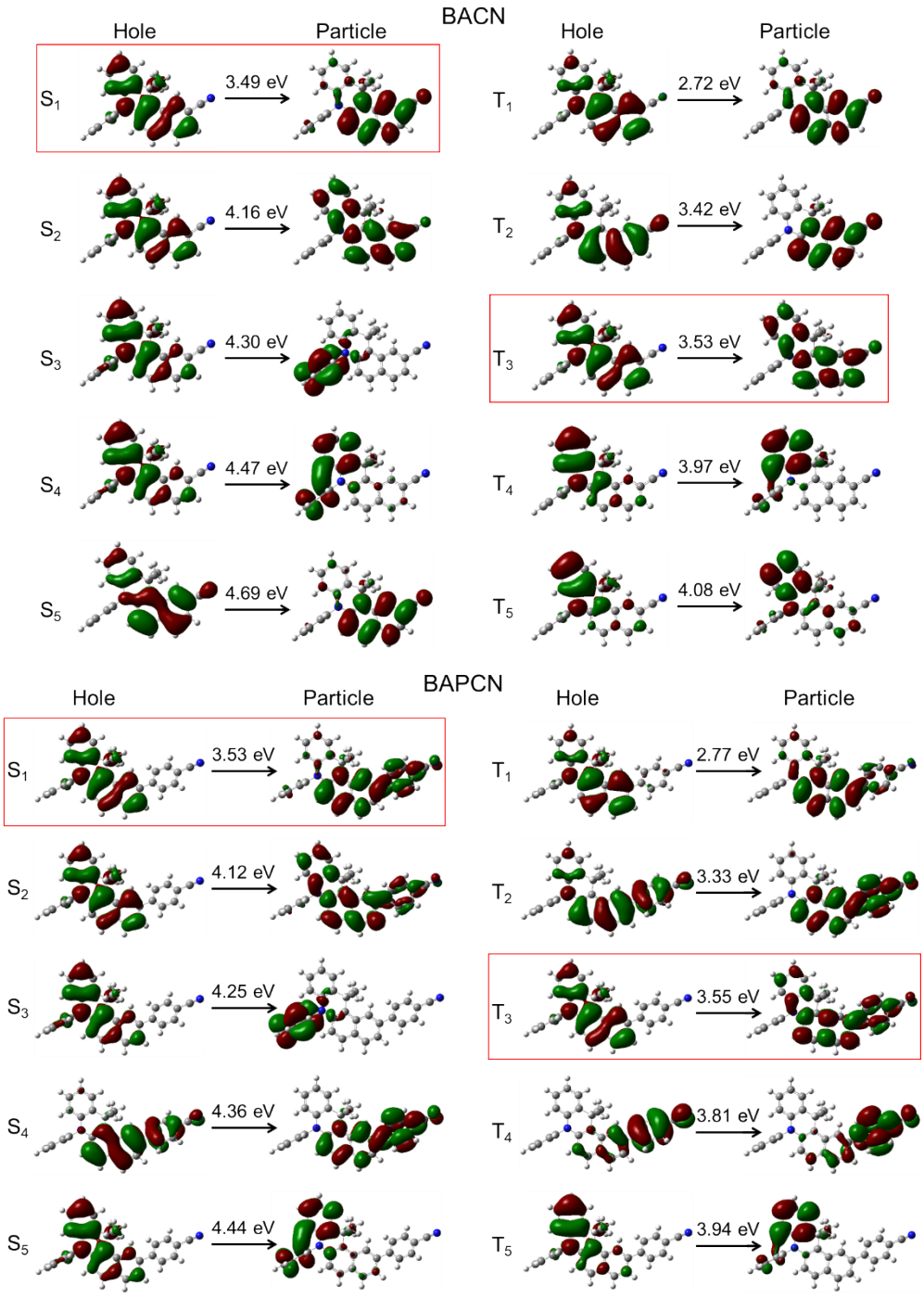

Fig. S7. The energy level (on the arrow) and the nature transition orbitals of the first five singlet and triplet states of BACN and BAPCN.

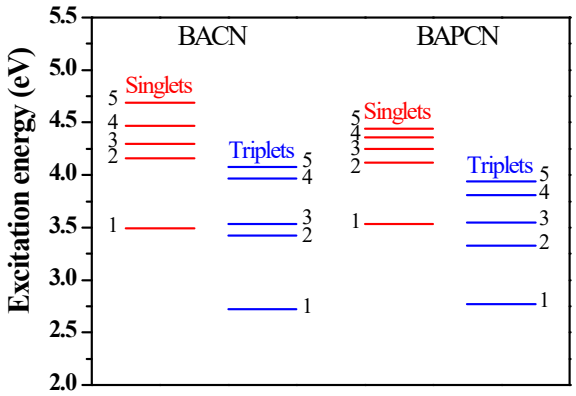

Fig. S8. Energy levels of the first five singlet and triplet excited states in BACN and BAPCN.

SI-6. Photophysical properties

Table S2. Detailed absorption and emission peak positions of BACN and BAPCN in different solvents.

Solvents	n	$f(\varepsilon, n)$	BACN			BAPCN		
			λ_{abs} [nm]	λ_{em} [nm]	ν_a-ν_f [cm^{-1}]	λ_{abs} [nm]	λ_{em} [nm]	ν_a-ν_f [cm^{-1}]
Hexane	1.375	0.0012	402	410	485	401	422	1241
Triethylamine	1.401	0.048	402	418	952	401	433	1843
Butyl ether	1.399	0.096	402	424	1291	401	440	2210
Isopropyl ether	1.368	0.145	402	426	1401	401	446	2516
Ethyl ether	1.352	0.167	402	430	1620	401	451	2765
Ethyl acetate	1.372	0.200	402	440	2148	401	468	3570
Tetrahydrofuran	1.407	0.210	402	441	2200	401	474	3841
Dichloromethane	1.424	0.217	402	449	2604	401	489	4488
Acetone	1.359	0.284	402	453	2801	401	496	4776
Acetonitrile	1.344	0.305	402	462	3231	401	510	5330

λ_{abs} = absorption maximum, λ_{em} = emission maximum, ν_a-ν_f = Stokes shift.

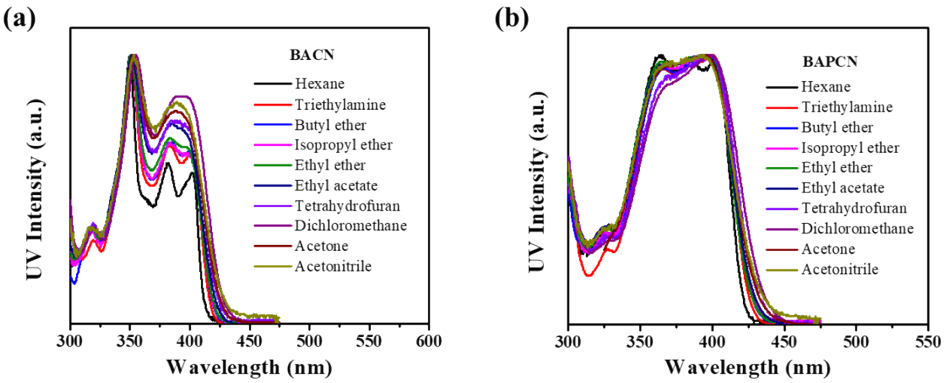

Fig. S9. The UV-vis absorption spectra of BACN and BAPCN in ten different solvents with increasing polarity.

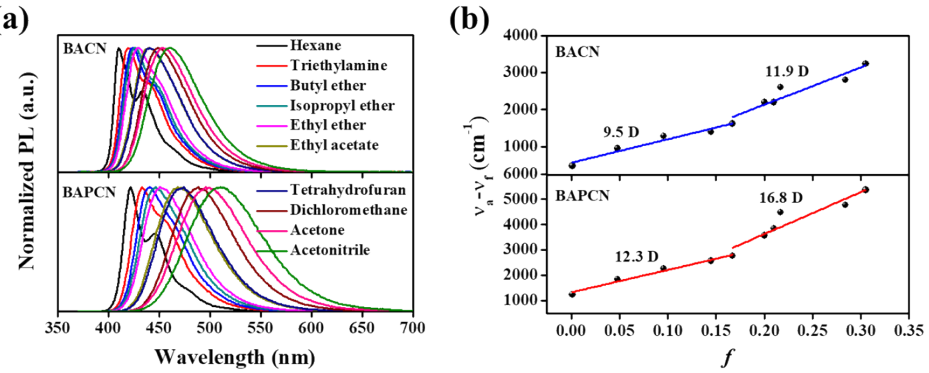

Fig. S10. (a) Normalized PL spectra of BACN and BAPCN measured in different solvents with increasing polarity. (b) Linear correlation of orientational polarization (*f*) of solvent media with the Stokes shift (ν_a-ν_f; a: absorbed light; f: fluorescence) for BACN and BAPCN.

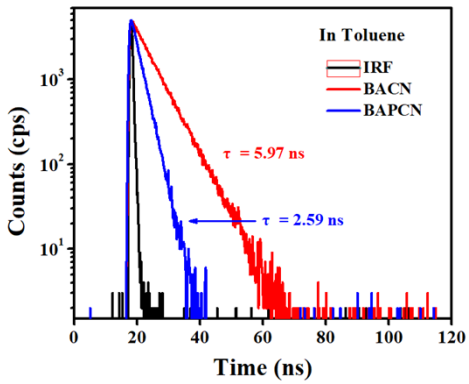

Fig. S11. Transient fluorescence decay spectra of BACN and BAPCN in dilute toluene (10^{-5} mol L^{-1}) at 300 K.

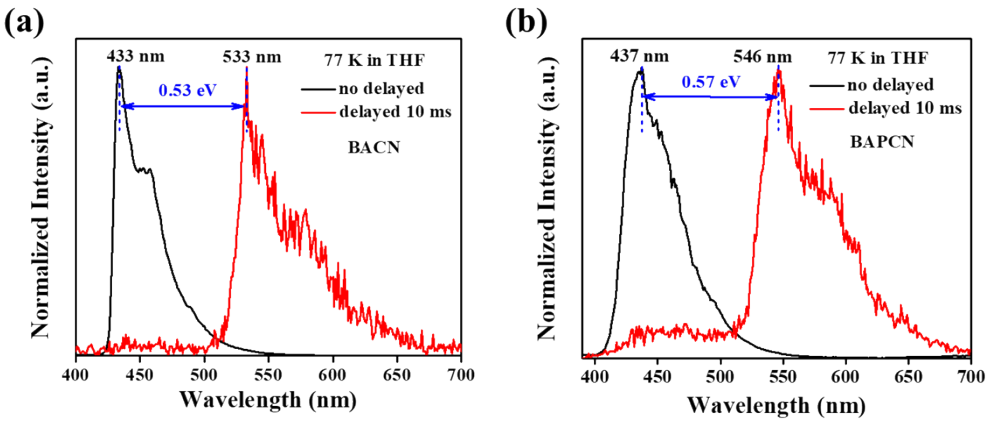

Fig. S12. The emission spectra at 77 K with and without a delay time of 10 ms of BACN and BAPCN in THF solutions.

The devices based on BACN and BAPCN all exhibited higher maximum EQE than the theoretical upper limit (5%) of traditional fluorescent materials (Table 2), and the radiative exciton utilization efficiency (EUE) broke the limit of 25% singlet excitons of spin statistics rule. Since the energy gaps between S_1 and T_1 of BACN and BAPCN are larger than 0.5 eV (Fig. S12), and the time-resolved fluorescence revealed mono-exponential decay with nano-scale lifetime (Fig. S11), the reverse intersystem crossing (RISC) from T_1 to S_1 seems cannot occur. Through the time-dependent DFT calculation (Fig. S8), we speculate that the breakthrough of EQE could ascribed to the RISC from upper excited states (*e.g.*, $T_2 \rightarrow S_1$) as we reported before.[1-5]

SI-7. Electroluminescence properties

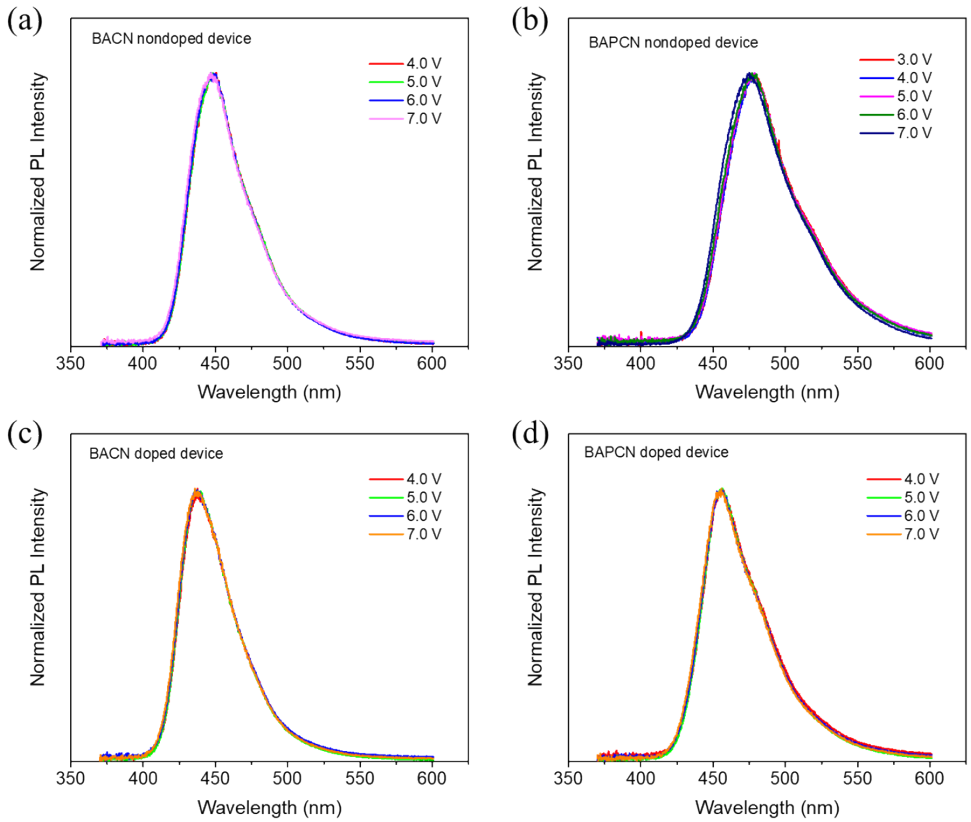

Fig. S13. EL spectra of BACN (a, c) and BAPCN (b, d) based devices at different voltages.

REFERENCES

(1) Li, W.; Pan, Y.; Xiao, R.; Peng, Q.; Zhang, S.; Ma, D.; Li, F.; Shen, F.; Wang, Y.; Yang, B.; Ma, Y. Employing ~100% Excitons in OLEDs by Utilizing a Fluorescent Molecule with Hybridized Local and Charge-Transfer Excited State. *Adv. Funct. Mater.* **2014,** *24*, 1609-1614.

(2) Li, W.; Pan, Y.; Yao, L.; Liu, H.; Zhang, S.; Wang, C.; Shen, F.; Lu, P.; Yang, B.; Ma, Y. A Hybridized Local and Charge-Transfer Excited State for Highly Efficient Fluorescent OLEDs: Molecular Design, Spectral Character, and Full Exciton Utilization. *Adv. Opt. Mater.* **2014,** *2*, 892-901.

(3) Wang, C.; Li, X.; Pan, Y.; Zhang, S.; Yao, L.; Bai, Q.; Li, W.; Lu, P.; Yang, B.; Su, S.; Ma, Y. Highly Efficient Nondoped Green Organic Light-Emitting Diodes with Combination of High Photoluminescence and High Exciton Utilization. *ACS Appl. Mater. Interfaces* **2016,** *8*, 3041-3049.

(4) Liang, X.; Wang, Z.; Wang, L.; Hanif, M.; Hu, D.; Su, S.; Xie, Z.; Gao, Y.; Yang, B.; Ma, Y. Tailoring Excited State Properties and Energy Levels Arrangement via Subtle Structural Design on D-π-A Materials. *Chinese J. Chem.* **2017,** *35*, 1559-1568.

(5) Xu, Y.; Liang, X.; Liang, Y.; Guo, X.; Hanif, M.; Zhou, J.; Zhou, X.; Wang, C.; Yao, J.; Zhao, R.; Hu, D.; Qiao, X.; Ma, D.; Ma, Y. Efficient Deep-Blue Fluorescent OLEDs with a High Exciton Utilization Efficiency from a Fully Twisted Phenanthroimidazole-Anthracene Emitter. *ACS Appl. Mater. Interfaces* **2019,** *11*, 31139-31146.